Scientific Report

TRANSPARENT PROCESS

EMBO reports

Arabidopsis MAKR5 is a positive effector of BAM3-dependent CLE45 signaling

Yeon Hee Kang & Christian S Hardtke*

Abstract

Receptor kinases convey diverse environmental and developmental inputs by sensing extracellular ligands. In plants, one group of receptor-like kinases (RLKs) is characterized by extracellular leucine-rich repeat (LRR) domains, which interact with various ligands that include the plant hormone brassinosteroid and peptides of the CLAVATA3/EMBRYO SURROUNDING REGION (CLE) type. For instance, the CLE45 peptide requires the LRR-RLK BARELY ANY MERISTEM 3 (BAM3) to prevent protophloem formation in *Arabidopsis* root meristems. Here, we show that other proposed CLE45 receptors, the two redundantly acting LRR-RLKs STERILITY-REGULATING KINASE MEMBER 1 (SKM1) and SKM2 (which perceive CLE45 in the context of pollen tube elongation), cannot substitute for BAM3 in the root. Moreover, we identify MEMBRANE-ASSOCIATED KINASE REGULATOR 5 (MAKR5) as a post-transcriptionally regulated amplifier of the CLE45 signal that acts downstream of BAM3. MAKR5 belongs to a small protein family whose prototypical member, BRI1 KINASE INHIBITOR 1, is an essentially negative regulator of brassinosteroid signaling. By contrast, MAKR5 is a positive effector of CLE45 signaling, revealing an unexpected diversity in the conceptual roles of *MAKR* genes in different signaling pathways.

Keywords CLE peptide; protophloem; receptor-like kinase; SKM1; SKM2
Subject Categories Plant Biology; Signal Transduction
DOI 10.15252/embr.201642450 | Received 29 March 2016 | Revised 28 May 2016 | Accepted 2 June 2016 | Published online 27 June 2016
EMBO Reports (2016) 17: 1145–1154

Introduction

Receptor-like kinases (RLKs) are abundant in *Arabidopsis*, where they convey various environmental and developmental inputs. One large group of RLKs is characterized by extracellular leucine-rich repeat (LRR) domains, which interact with various ligand types [1]. These comprise secreted, endogenous molecules, such as brassinosteroid plant hormones or peptide ligands of the CLAVATA3/EMBRYO SURROUNDING REGION (CLE) family. Among the various pathways, brassinosteroid perception is by far the best characterized [2]. Brassinosteroids interact with the receptor kinase BRASSINOSTEROID INSENSITIVE 1 (BRI1) [3], which stabilizes BRI1 interaction with its co-receptor and triggers an intracellular signaling cascade that transmits the signal to nuclear effectors [2,4–7]. A critical early signaling component is BRI1 KINASE INHIBITOR 1 (BKI1), which interacts with BRI1 and dampens its activity when brassinosteroid levels are low [8]. BKI1 is thus mostly plasma membrane-associated, but rapidly dissociates into the cytoplasm upon brassinosteroid treatment, thereby releasing BRI1 inhibition [8,9]. In the cytoplasm, BKI1 can interact with 14-3-3 proteins, which reinforces its cytoplasmic localization and possibly also facilitates signal transduction because 14-3-3 proteins inhibit downstream transcription factor targets of brassinosteroid signaling [10]. However, because BKI1 gain-of-function inhibits brassinosteroid signaling while its loss-of-function confers brassinosteroid hypersensitivity, BKI1 is considered an essentially negative regulator of the pathway [8–11]. BKI1 is the founding member of a small family that comprises six additional proteins named MEMBRANE-ASSOCIATED KINASE REGULATOR (MAKR) 1–6 [9]. Besides BKI1, next to nothing is known about signaling pathways and developmental processes that require *MAKR* gene activity. The only exception is *MAKR4*, which has been implicated in lateral root formation [12].

Although a number of (putative) CLE ligand/LRR-RLK pairs have been defined in various developmental processes, comparatively little is known about their downstream signaling components [13]. At least in part, this might be due to redundancies in signaling intermediates and their sharing by distinct pathways, which also complicates their genetic identification. Moreover, a given ligand might be perceived by different LRR-RLKs, depending on affinities, expression patterns, and expression levels. For example, the dodecapeptide CLE45 has been described as a powerful agent to suppress the formation of root protophloem sieve elements [14]. This effect requires the LRR-RLK BARELY ANY MERISTEM 3 (BAM3), which, similar to *CLE45*, is expressed in the developing protophloem [15]. CLE45 and BAM3 are thought to constitute an endocrine signaling module that redundantly prevents premature differentiation of developing sieve elements [16]. However, CLE45 was also found to prolong pollen tube growth at high temperature, and two redundantly acting LRR-RLKs, STERILITY-REGULATING KINASE MEMBER 1 (SKM1) and SKM2, presumably act as CLE45 receptors in this process [17].

In the protophloem context, the CLE45-BAM3 module was identified through a second site suppressor screen for loss-of-function of

Department of Plant Molecular Biology, University of Lausanne, Lausanne, Switzerland
*Corresponding author. Tel: +41 21 692 4251; E-mail: christian.hardtke@unil.ch

the positive regulator of protophloem sieve element differentiation, *BREVIS RADIX* (*BRX*) [15]. *brx* null mutants display severely reduced root growth and associated systemic phenotypes that can be traced to a local defect in sieve element differentiation [14,16]. In *brx* mutants, protophloem precursor cells frequently fail to differentiate. These so-called gap cells can be identified in confocal microscopy because of their morphological features, such as the absence of a reinforced cell wall [16,18]. Second site *BAM3* loss-of-function completely rescues these *brx* phenotypes [15]. Here, we show that loss-of-function in *MAKR5* partially suppresses *brx* phenotypes because MAKR5 is an amplifier of BAM3-dependent CLE45 signaling. Therefore, unlike the prototypical member of the MAKR protein family, BKI1, which is an essentially negative regulator of brassinosteroid signaling, MAKR5 is a positive effector of CLE45 signaling.

Results and Discussion

SKM1 and SKM2 cannot substitute for BAM3 in the root

In our attempts to further characterize BAM3-dependent CLE45 perception in root protophloem development, we sought to clarify whether SKM1 or SKM2 act redundantly with, or possibly as co-receptors of BAM3 in this context. Both *SKM1* and *SKM2* are expressed in the root as revealed by respective reporter transgenes; however, expression was apparently absent from the meristem, where the protophloem is formed (Fig 1A and B). Whereas *SKM2* expression was detected largely throughout the root starting from the transition zone (Fig 1B), *SKM1* expression was restricted to the more mature vasculature (Fig 1A). Thus, *BAM3* expression (Fig EV1A) does not coincide with *SKM1* or *SKM2* expression in the root tip. Consistently, transgenic expression of the *BAM3* coding sequence under control of the *SKM1* promoter could not restore CLE45 sensitivity in a *bam3* null mutant (Fig 1C). Further corroborating these observations, neither *skm1* or *skm2* single mutants, nor the *skm1 skm2* double mutant displayed any resistance to the effects of external CLE45 application (Fig 1D). Finally, when ectopically expressed under control of the *BAM3* promoter, neither *SKM1* nor *SKM2* could restore CLE45 sensitivity in a *bam3* mutant (Fig 1E), or restore a *brx* phenotype when introduced into a *bam3 brx* double mutant, unlike a similar construct with the *BAM3* coding sequence (Fig EV1B). In summary, our results suggest that SKM1 and SKM2 are not required for CLE45 perception in the root and also cannot replace BAM3.

Second site *MAKR5* loss-of-function partially suppresses *brx* phenotypes

Further insight into CLE45 signaling was obtained from our *brx* second site suppressor screen. We identified a partially suppressed *brx* mutant (Fig 2A), in which root growth and root meristem size were rescued from ~40 and ~50% of wild type, respectively, to ~80 and ~90% (Fig 2B and C). Whole genome sequencing of DNA from bulked segregant pools of individuals with fully penetrant mutant or suppressed phenotype (obtained from a backcross to the *brx* parental line) suggested an early stop codon (W10*) in *MAKR5* (At5g52870) as the causative second site. Both *MAKR5::MAKR5* and *MAKR5::MAKR5-GFP* transgenes restored the *brx* phenotype when introduced in this *brx makr5* double mutant (Fig 2A), confirming *makr5* as the causative locus and demonstrating that MAKR5-GFP fusion protein is fully functional. Rescue of root meristem size was also apparent at the cellular level (Fig 2D), and physiological

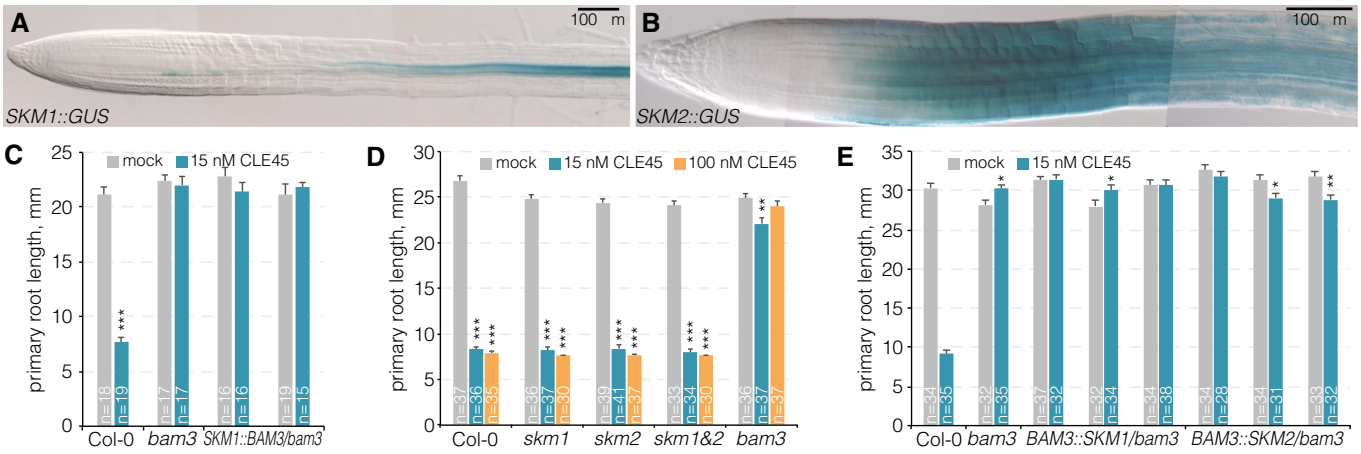

Figure 1. SKM1 and SKM2 do not play a role in CLE45 perception in the root.

A, B Expression patterns (blue stain) of GUS reporter genes driven by the *SKM1* (A) or *SKM2* (B) promoter in roots of 5-day-old Col-0 seedlings.

C Non-complementation of CLE45 insensitivity of the *bam3* mutant by *BAM3* expressed under control of the *SKM1* promoter (7-day-old seedlings; 2 independent transgenic lines per construct are shown).

D Full CLE45 sensitivity of *skm1* or *skm2* single- and double-mutant roots (7-day-old seedlings).

E Failure of *SKM1* or *SKM2* expressed under control of the *BAM3* promoter to complement CLE45 insensitivity of the *bam3* mutant (7-day-old seedlings; 3 independent transgenic lines per construct are shown).

Data information: Differences as compared to mock are not statistically significant unless indicated (Student's *t*-test); *$P < 0.05$; **$P < 0.01$; ***$P < 0.001$; error bars indicate standard error of the mean.

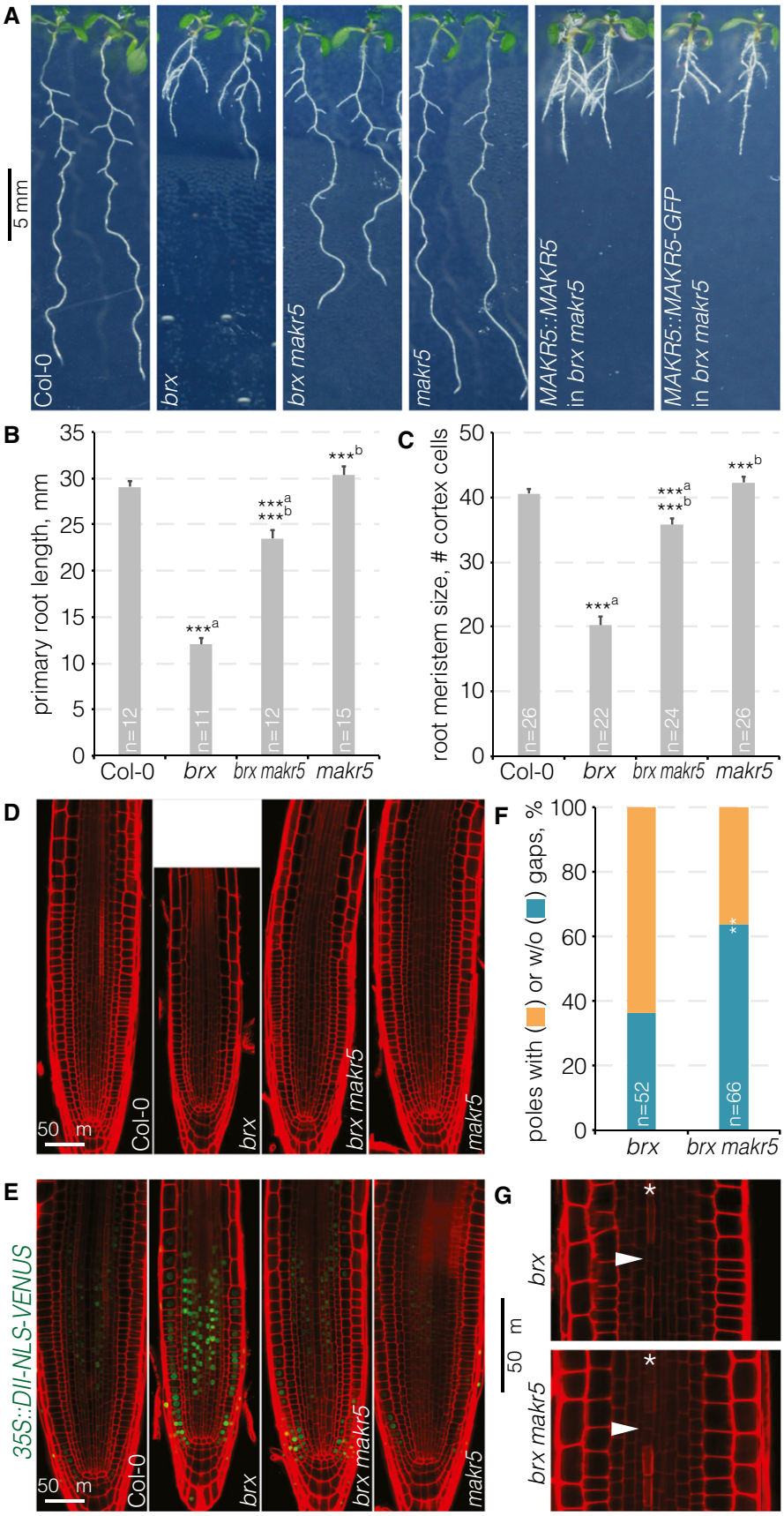

Figure 2.

Figure 2. Second site mutation in *MAKR5* partially suppresses *brx* root phenotypes.

A Root phenotypes of 7-day-old seedlings of the indicated genotypes.
B Primary root length of 7-day-old seedlings.
C Root meristem size in 5-day-old seedlings.
D Root meristem phenotype of 5-day-old seedlings, confocal microscopy, propidium iodide-stained (red).
E Auxin activity as visualized by the constitutively expressed inverse DII-NLS-VENUS marker (green) in root meristems of 5-day-old seedlings.
F Gap cell frequency in *brx* single or *brx makr5* double mutants (note: gap cells were absent from Col-0 wild type or *makr5* single mutants).
G Illustration of gap cells (arrowheads) in developing protophloem sieve element strands (asterisks) of *brx* single or *brx makr5* double mutants.

Data information: Differences are not statistically significant unless indicated. (B, C): Student's *t*-test; (F): Fisher's exact test; (B, C): [a]: versus Col-0; [b]: versus *brx*; $^{**}P < 0.01$; $^{***}P < 0.001$; error bars indicate standard error of the mean.

phenotypes, such as reduced auxin signaling throughout *brx* meristems, were likewise largely restored by *makr5* second site mutation (Fig 2E). Finally, *brx* sieve element differentiation defects were also partially rescued, leading to a significant reduction in gap cell frequency (Fig 2F and G). The *makr5* single mutant, segregated from the *brx makr5* double mutant after repeated backcrossing to the Col-0 wild-type background, appeared morphologically normal (Fig 2A–E). To exclude the possibility that *makr5* rescue of *brx* is indirect, we introduced a reporter gene for *BRX-LIKE 1* (*BRXL1*) into the *brx makr5* double mutant. *BRXL1* is the only *Arabidopsis* homolog that can substitute for *BRX* when expressed ectopically in the protophloem [19,20]. However, *BRXL1* expression was unchanged in the *brx makr5* mutant (Fig EV1C). The data thus suggest a direct role of *MAKR5* loss-of-function in *brx*-related phenotypes.

MAKR5 loss-of-function confers reduced CLE45 sensitivity

The absence of apparent morphological phenotypes in the *makr5* mutant is similar to *bam3* mutants, which are, however, resistant to the effects of externally applied CLE45 (Fig 1D) [15]. Given the importance of the CLE45-BAM3 module in antagonizing *BRX* activity [14], we thus tested whether *makr5* mutants are possibly CLE45 resistant. Indeed, *makr5* mutants were insensitive to CLE45 levels that strongly suppressed root growth in wild type (Fig 3A). As expected, this extended to protophloem sieve element differentiation, which was fully suppressed in CLE45-treated Col-0 wild-type background, but not in *makr5* mutant seedlings (Fig 3B and C). However, reflecting partial versus full rescue of *brx* by *makr5* or *bam3* mutation, respectively, *makr5* seedlings were not as CLE45 resistant as *bam3* seedlings, which were entirely insensitive to much higher CLE45 levels (Fig 3A). The data therefore suggest a substantial, yet partial requirement of *MAKR5* for CLE45 signaling.

Consistent with a role of MAKR5 in CLE45 perception, transcriptional reporters indicated *MAKR5* expression in the vascular cylinder throughout the root (Fig 3D). Expression started early in the meristem and was detectable in the procambial cells and the phloem poles, but apparently absent from the xylem axis (Fig 3E). By comparison, expression of MAKR5-GFP fusion protein under control of the same native *MAKR5* promoter was more constrained (Fig 3F). MAKR5-GFP was hardly detectable in procambial cells and most abundant in the cell files surrounding the protophloem sieve element strands, that is, the metaphloem, companion cell, and phloem pole pericycle files (Fig 3G). However, MAKR5-GFP was also clearly detectable, although less abundant, in developing sieve elements. The developing sieve elements were also confirmed as MAKR5 site of action because *MAKR5* expressed under control of the sieve element-specific *COTYLEDON VASCULAR PATTERN 2* (*CVP2*) promoter could complement the *makr5* mutant, unlike expression under control of the companion cell-specific *SUCROSE TRANSPORTER 2* (*SUC2*) promoter (Fig 3H). At the subcellular level, MAKR5-GFP displayed cytosolic as well as plasma membrane-associated localization (Fig 3I). In summary, the data suggest that *MAKR5* is expressed in all cell files of the vascular cylinder except the xylem, and including the CLE45 site of action, the protophloem. Moreover, MAKR5 might be subject to post-transcriptional or post-translational regulation, since MAKR5-GFP fusion protein appeared to be less stable in procambial than in phloem pole cells.

MAKR5 specificity for relay of the CLE45 signal resides in its C-terminus

The MAKR protein family has been defined by its homology to BKI1, which is mainly based on the presence of a few conserved motifs. They comprise a K/R-rich putative membrane hook motif that is spread throughout the otherwise loosely homologous center of MAKR proteins, and a more similar, S-rich C-terminus (Fig 4A), which includes a conserved motif that is responsible for BRI1 interaction in BKI1 [9]. To define functional domains of MAKR5, we first investigated CITRINE fusions of truncated MAKR5 derivatives ($MAKR5^{1–110}$, $MAKR5^{1–206}$, $MAKR5^{101–230}$, and $MAKR5^{207–326}$) (Fig 4A) expressed in the same regulatory context under control of the *MAKR5* promoter in *makr5* background. All fusion proteins were expressed at roughly similar levels as full-length MAKR5-GFP and showed stronger expression at the phloem pole, with the exception of the C-terminal $MAKR5^{207–326}$ fragment (Fig 4B). These observations were consistent across multiple independent transgenic lines (8–14 per construct were analyzed in detail). At the subcellular level, only the two fragments that contained the membrane hook motif ($MAKR5^{1–206}$ and $MAKR5^{101–230}$) displayed clear plasma membrane association, corroborating the hook's functional importance. By contrast, $MAKR5^{1–110}$ was mostly, and $MAKR5^{207–326}$, exclusively cytosolic (Fig 4B). Investigation of corresponding CITRINE fusions ectopically expressed under control of the ubiquitous *UBIQUITIN 10* (*UBQ10*) promoter confirmed these observations (Fig 4C). Interestingly, unlike what has been reported for BKI1 overexpression [8,9], MAKR5 overexpression (Fig EV1D) had no apparent dominant effects and also could not restore CLE45 sensitivity in a *bam3* background (Fig EV1E). Thus, MAKR5 is necessary but not sufficient to confer full CLE45 sensitivity. Moreover, the finding that

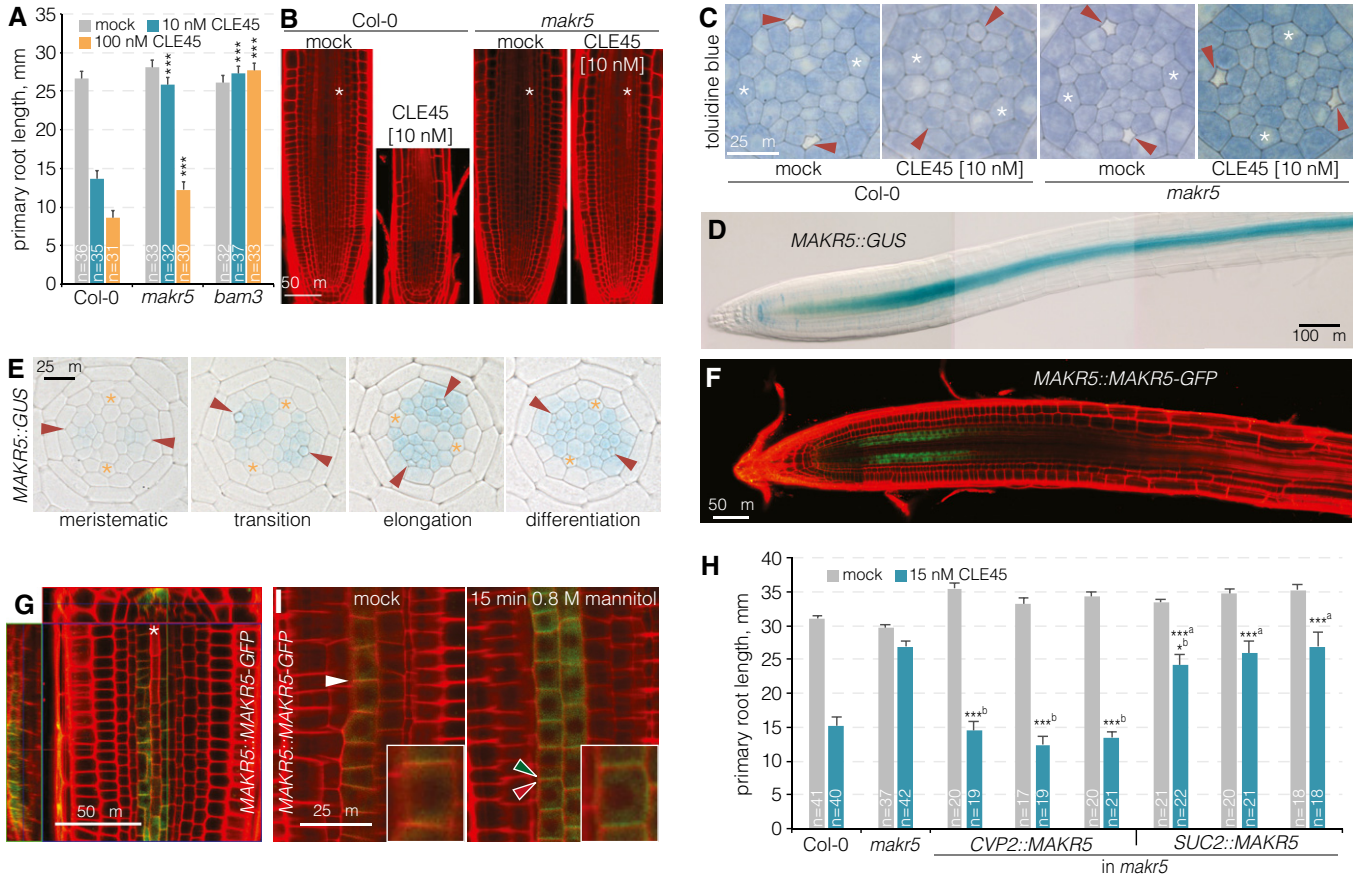

Figure 3. *MAKR5* loss-of-function confers CLE45 resistance.

A Primary root length of 7-day-old seedlings of the indicated genotypes in response to continuous CLE45 treatments.

B Root meristem phenotypes of (CLE45-treated) 5-day-old seedlings (asterisks: protophloem sieve element strands). Note absence of protophloem in CLE45-treated Col-0 wild-type roots.

C Transverse sections of (CLE45-treated) 5-day-old roots, just before the onset of protoxylem (asterisks) differentiation. Note failure of protophloem sieve elements (arrowheads) to differentiate in CLE45-treated Col-0 (indicated by dense cytoplasm).

D Expression pattern of GUS reporter gene driven by the *MAKR5* promoter in roots of 5-day-old Col-0 seedlings.

E Corresponding transverse sections from different positions along the root meristem (asterisks: protoxylem cells; arrowheads: protophloem poles).

F Expression of a MAKR5-GFP fusion protein under control of the *MAKR5* promoter in roots of 5-day-old seedlings.

G Corresponding optical sections illustrating MAKR5-GFP expression in developing protophloem sieve elements (asterisk) and adjacent cell files.

H Complementation of *makr5* CLE45 insensitivity by *MAKR5* expression under control of a promoter specific for developing sieve elements (*CVP2*), but not by expression under control of a companion cell-specific promoter (*SUC2*) (7-day-old seedlings; 3 independent transgenic lines per construct are shown).

I Subcellular localization of MAKR5-GFP (meristematic zone). Note plasma membrane association (white, green arrowheads) and dissociation from the cell wall (red arrowhead) upon osmosis.

Data information: Differences are not statistically significant unless indicated (Student's *t*-test); *$P < 0.05$; ***$P < 0.001$; (A): versus Col-0; (H): [a]: versus CLE45-treated Col-0; [b]: versus CLE45-treated *makr5*; error bars indicate standard error of the mean.

Figure 4. Specificity for CLE45 signal transduction resides in the MAKR5 C-terminus.

A Schematic presentation of the MAKR5 protein, indicating the K/R-rich membrane hook motif, the S-rich conserved C-terminus, the position of the *makr5* mutation, and the truncated fragments tested.

B Expression of truncated MAKR5 fusion proteins under control of the *MAKR5* promoter in 5-day-old roots (asterisks: protophloem sieve element strands).

C Close-up of protophloem sieve element strands expressing truncated MAKR5-CITRINE fusion proteins under control of the *UBQ10* promoter (asterisks: protophloem sieve element strands).

D Failure of truncated MAKR5 fusion proteins to complement CLE45 insensitivity of the *makr5* mutant (7-day-old seedlings; 1-2 independent transgenic lines per construct are shown).

E Sensitivity of *makr5* mutant roots to continuous brassinolide (BL) treatment (7-day-old seedlings).

F Expression of MAKR5-BKI1 fusion proteins under control of the *MAKR5* promoter in roots of 5-day-old *makr5* seedlings (asterisks: protophloem sieve element strands).

G Complementation of CLE45 insensitivity of *makr5* roots by BKI1-MAKR5, but not MAKR5-BKI1 fusion protein (7-day-old seedlings; 3 independent transgenic lines per construct are shown).

Data information: Differences are not statistically significant unless indicated (Student's *t*-test); *$P < 0.05$; **$P < 0.01$; ***$P < 0.001$; (D, G): [a]: versus mock; [b]: versus *makr5*; (E): versus Col-0; error bars indicate standard error of the mean.

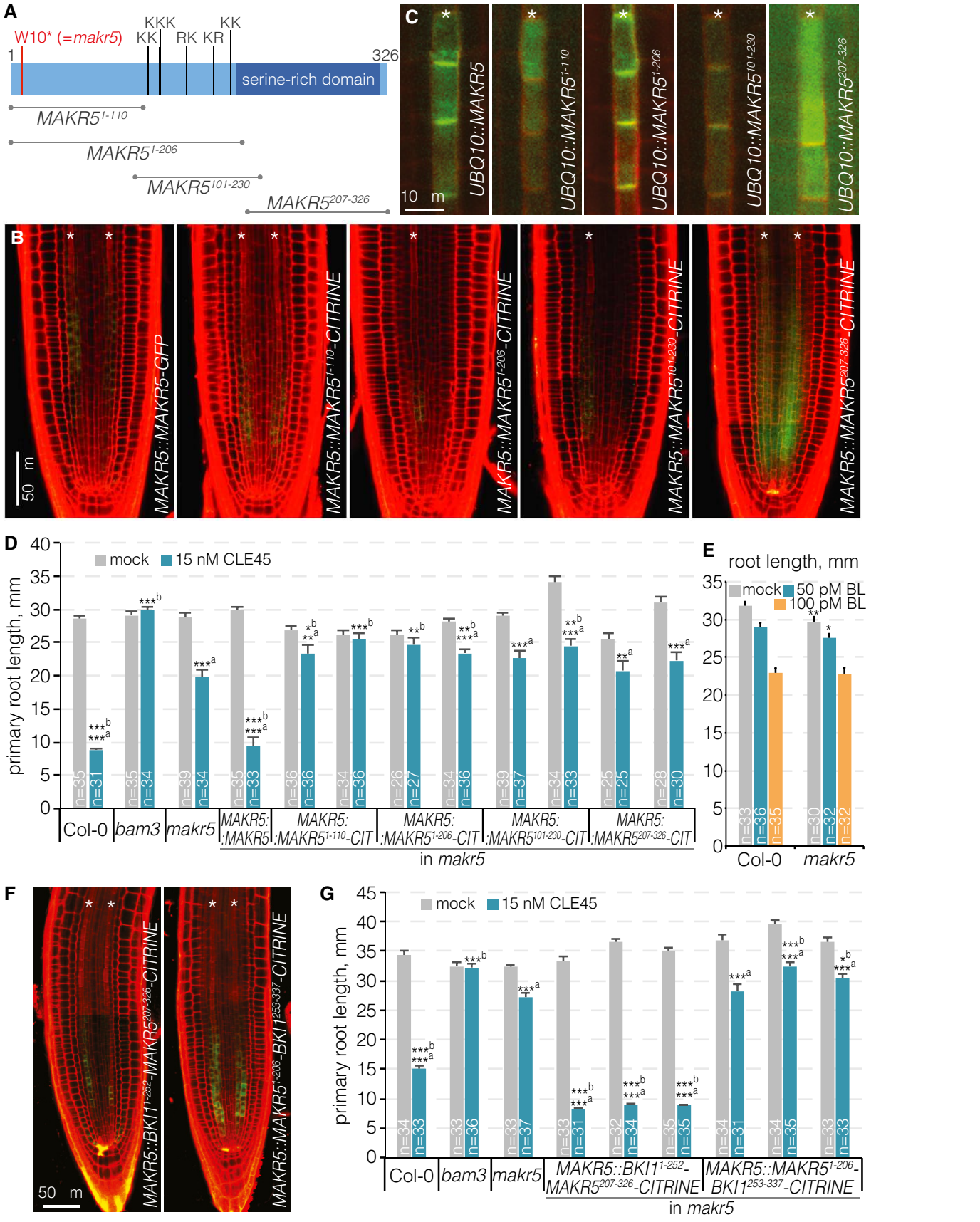

Figure 4.

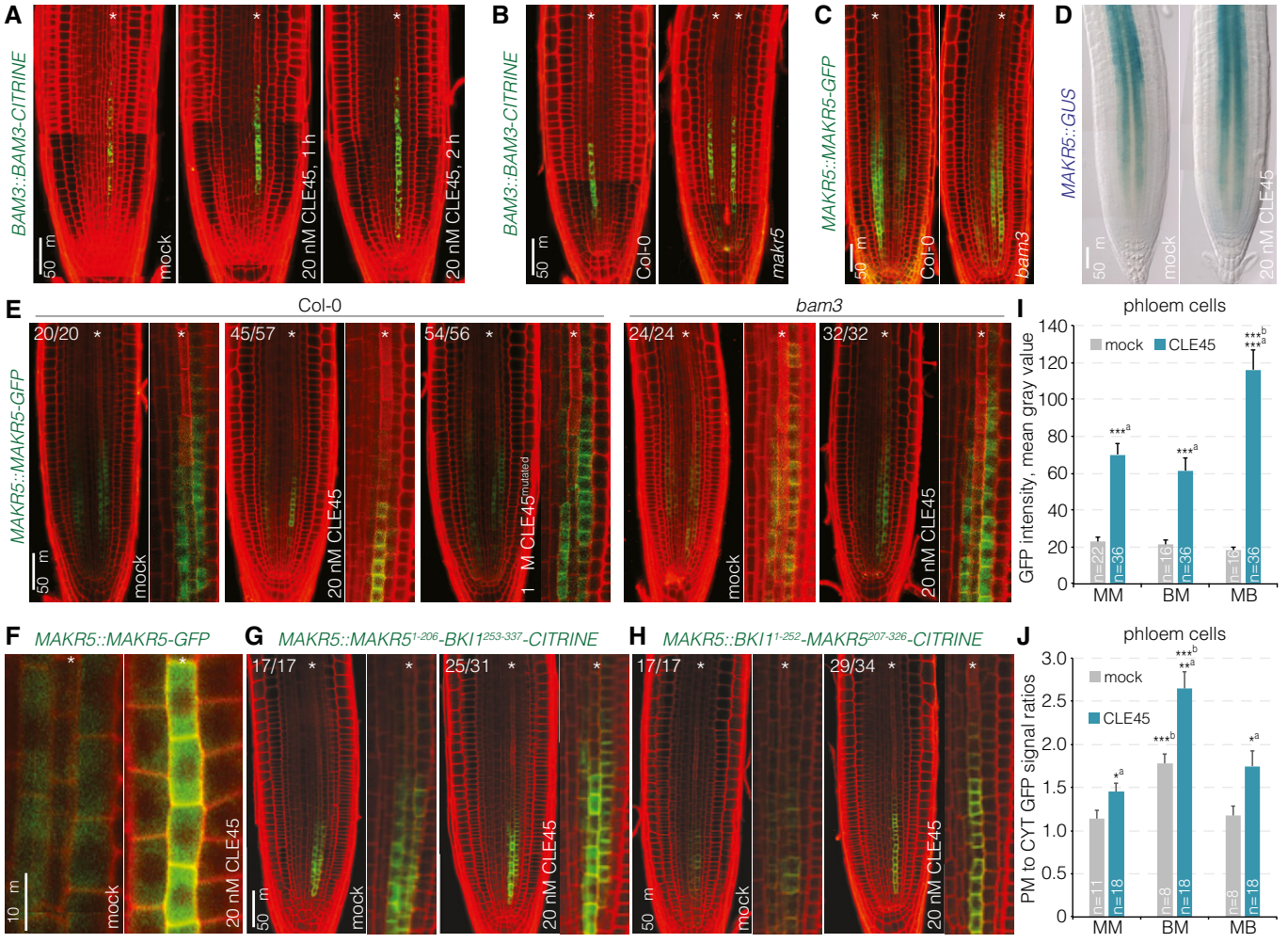

Figure 5. Post-transcriptional regulation of MAKR5 by CLE45 treatment.

A Increased expression of BAM3-CITRINE fusion protein under control of the *BAM3* promoter in developing protophloem sieve elements (asterisks) of 5-day-old *bam3* roots upon CLE45 treatment.

B Expression of BAM3-CITRINE fusion protein under control of the *BAM3* promoter in 5-day-old Col-0 roots or *makr5* roots (asterisks: protophloem sieve element strands).

C Expression of MAKR5-GFP fusion protein under control of the *MAKR5* promoter in 5-day-old Col-0 or *bam3* roots (asterisks: protophloem sieve element strands).

D GUS reporter gene expression driven by the *MAKR5* promoter in roots of 5-day-old Col-0 seedlings upon CLE45 treatment.

E Expression of MAKR5-GFP fusion protein under control of the *MAKR5* promoter in 5-day-old roots upon CLE45 treatment (3 h). Note accumulation of MAKR5-GFP in protophloem sieve elements (magnified) and its dependence on functional BAM3 and CLE45. The frequency of representative observations per total observations is indicated (asterisks: protophloem sieve element strands).

F Close-up view of MAKR5-GFP accumulation in the protophloem cell file upon CLE45 treatment (asterisks: protophloem sieve element strands).

G, H Accumulation of MAKR5-BKI1 fusion proteins in protophloem cells upon CLE45 treatment. The frequency of representative observations per total observations is indicated (asterisks: protophloem sieve element strands).

I, J Quantification of fusion protein abundance in developing protophloem cells upon expression under control of the *MAKR5* promoter, showing mean total fluorescence (I) and plasma membrane to cytosol signal ratio (J). MM: MAKR5-GFP; BM: BKI1$^{1–252}$-MAKR5$^{207–326}$-CITRINE; MB: MAKR5$^{1–206}$-BKI1$^{253–337}$-CITRINE; Differences versus mock are not statistically significant unless indicated (Student's *t*-test); [a]: versus mock; [b]: versus MAKR5-GFP; $*P < 0.05$; $**P < 0.01$; $***P < 0.001$; error bars indicate standard error of the mean.

MAKR5$^{207–326}$-CITRINE was also more abundant than the other fragments when expressed under the same constitutive promoter suggests that the N-terminal two-thirds of MAKR5 might contain destabilizing motifs. Such motifs could be responsible for the decreased MAKR5 abundance in non-phloem pole cell files. Finally, the data also suggest that full integrity of the MAKR5 protein is required for its function, since none of the fragments could complement the *makr5* mutant (Fig 4D).

To determine which MAKR5 domains are responsible for its specific activity, we next tested the propensity of hybrid protein fusions to complement the *makr5* mutant. Because *makr5* has a wild-type response to brassinosteroids (Fig 4E), we chose BKI1 for domain swaps. In one construct, the MAKR5$^{1–206}$ N-terminus including the membrane hook motif was fused to the BKI1$^{253–337}$ C-terminus (encompassing the S-rich C-terminus and the BRI1 interaction domain), while in another, complementary construct the

BKI1$^{1–252}$ N-terminus (including the membrane hook) was fused to the MAKR5$^{207–326}$ C-terminus. Both fusions were expressed under control of the *MAKR5* promoter and displayed the enhanced expression in the phloem pole cell files (Fig 4F). However, the MAKR5$^{1–206}$-BKI1$^{253–337}$-CITRINE fusion protein appeared to be more stable than its BKI1$^{1–252}$-MAKR5$^{207–326}$-CITRINE counterpart. Yet, the MAKR5$^{1–206}$-BKI1$^{253–337}$-CITRINE fusion could not complement the *makr5* mutant (Fig 4G) or restore the *brx makr5* phenotype (Fig EV1F), while the BKI1$^{1–252}$-MAKR5$^{207–326}$-CITRINE fusion could. Therefore, the data suggest that MAKR5 specificity for the CLE45 pathway resides in its C-terminus.

CLE45 signaling positively regulates MAKR5 activity in a post-transcriptional manner

Feedback and feed forward phenomena are frequent in signaling pathways, as exemplified by the positive effect of CLE45 treatment on *BAM3* gene expression [15], which also leads to BAM3 protein accumulation (Fig 5A). Expression of a *BAM3* transcriptional reporter was, however, not markedly reduced in *makr5* (Fig EV1A and G), as was the abundance of BAM3-CITRINE fusion protein (Fig 5B), which might reflect the fact that *MAKR5* is only partially required for CLE45 perception. Conversely, *bam3* mutation had no detectable robust impact on MAKR5-GFP fusion protein abundance or localization (Fig 5C), which was consistent with CLE45 insensitivity of *MAKR5* transcription (Fig 5D). However, CLE45 application triggered a strong accumulation of MAKR5-GFP in developing sieve elements (Fig 5E). At the same time, MAKR5-GFP plasma membrane association appeared to increase. This response was saturated at the low nanomolar CLE45 concentrations that trigger a full phenotypic response (Fig EV1H). Moreover, it did not occur in the absence of functional *BAM3* (Fig 5E) or in response to a mutated, inactive CLE45 derivative (Figs 5E and EV1I and J). The data thus suggest that MAKR5 protein is recruited to the plasma membrane and possibly stabilized upon CLE45 perception in developing sieve elements (Fig 5F). However, we could not detect interaction of MAKR5 with the BAM3 kinase domain in yeast two-hybrid or alternative assays (Fig EV1K and L). This could mean that other, still unidentified players are involved in this response, for example, a BAM3 co-receptor or downstream signaling components, or that interaction could be very transient.

The protophloem accumulation feature was retained in the MAKR5$^{1–206}$-BKI1$^{253–337}$-CITRINE and BKI1$^{1–252}$-MAKR5$^{207–326}$-CITRINE fusion proteins (Fig 5G and H), and again the MAKR5$^{1–206}$-BKI1$^{253–337}$-CITRINE fusion appeared to be more stable in this assay than its BKI1$^{1–252}$-MAKR5$^{207–326}$-CITRINE counterpart. In general, quantification of these otherwise visually robust observations proved difficult because of the very low expression level of *MAKR5*. However, the protophloem accumulation offered an opportunity to gauge relative levels despite this limitation. In developing protophloem cells of parallel-grown *MAKR5::MAKR5-GFP*, *MAKR5::MAKR5$^{1–206}$-BKI1$^{253–337}$-CITRINE* and *MAKR5::BKI1$^{1–252}$-MAKR5$^{207–326}$-CITRINE* lines, fusion protein intensity was comparable in mock conditions but increased upon CLE45 treatment (Fig 5I). This increase was substantially higher for MAKR5$^{1–206}$-BKI1$^{253–337}$-CITRINE (~6-fold) than for the other two fusions (~3-fold). Concomitantly, the ratio of plasma membrane-associated to cytosolic signal increased (Fig 5J), and this ratio was higher in both mock and CLE45 condition for BKI1$^{1–252}$-MAKR5$^{207–326}$-CITRINE as compared to the other two proteins. These observations corroborate that the N-termini of MAKR5 and BKI1 are interchangeable, but also suggest that the BKI1 N-terminus confers comparatively stronger plasma membrane association. Moreover, given the increased stability of the isolated MAKR5 C-terminus (Fig 4B), and of the non-functional MAKR5$^{1–206}$-BKI1$^{253–337}$-CITRINE fusion as compared to the functional BKI1$^{1–252}$-MAKR5$^{207–326}$-CITRINE fusion, the results also suggest that MAKR5 protein is turned over upon signal transduction.

Conclusion

In summary, our data suggest that *MAKR5* is required for full perception of the BAM3-dependent CLE45 signal. The dynamic behavior of MAKR5 protein in response to CLE45 treatment suggests that this involves post-transcriptional events, which promote its plasma membrane association. In this respect, MAKR5 behaves distinct from the prototypical MAKR family protein BKI1. Moreover, while BKI1 is an essentially negative regulator of brassinosteroid signaling, MAKR5 is a positive effector and amplifier of CLE45 signaling, revealing an unexpected diversity in the conceptual roles of *MAKR* genes in different signaling pathways.

Materials and Methods

Plant materials, growth conditions, and physiological assays

All mutant and wild-type materials were in the *Arabidopsis* Columbia-0 (Col-0) standard background. The *bam3-2*, *skm1*, and *skm2* null mutant alleles, and the *BRXL1::GUS*, *35S::DII-NLS-VENUS*, and *BAM3::BAM3-CITRINE* transgenic lines have been described previously [14,17,20–22]. For plant tissue culture, seeds were surface-sterilized, germinated, and grown vertically on half strength MS agar media under continuous light at 22°C. CLE45 peptide and brassinolide treatments were performed according to standard procedures as previously described [15,23]. To create an inactive CLE45 derivative, the last three amino acids were replaced by alanines. For visualization of GUS reporter activity, 5-day-old seedlings were incubated in X-gluc staining buffer solution at 37°C for 1 h in darkness. For plasmolysis, 5-day-old *MAKR5::MAKR5-GFP* seedlings were incubated in 0.8 M mannitol solution for 15 min as previously described [24].

Microscopy

To visualize fluorescent proteins, seedlings were stained with propidium iodide (PI) and examined under a Zeiss LSM700 inverted confocal microscope, with excitation at 488 nm and detection with a 490- to 500-nm band path filter for GFP and CITRINE, and excitation at 555 nm and detection with a 560-nm long-path filter for PI. For GUS reporter line transverse sections, roots were embedded in plastic resin, sectioned, and stained with 0.1% toluidine blue, then visualized using a Leica DM5500 compound microscope, essentially as described [14]. For presentation, composite images had to be assembled in various instances.

Constructs and generation of transgenic lines

Binary constructs were created with Gateway Cloning Technology (Invitrogen). For *MAKR5::GUS*, *SKM1::GUS*, and *SKM2::GUS*, corresponding 2-kb 5′ flanking DNA promoter fragments were amplified by PCR and introduced into binary vector pMDC163 (*MAKR5*) or pH7m24GW (*SKM1 & 2*). For *MAKR5::MAKR5* and *MAKR5::MAKR5-GFP* (mGFP6 version), the genomic DNA fragment spanning the *MAKR5* gene and its 2-kb 5′ flanking region was amplified and introduced into binary vector pMDC99 and pMDC107, respectively. *SKM1* gene fragments were amplified from genomic DNA templates, and *SKM2* coding sequence was amplified from cDNA templates. For the *MAKR5* deletion constructs, truncated MAKR5 coding sequence fragments were amplified. For the *MAKR5-BKI1* fusion constructs, corresponding fragments were obtained by gene synthesis (GeneArt). To obtain CITRINE fusion proteins, fragments were cloned into vector pH7mGW34. All binary constructs were introduced into *Agrobacterium tumefaciens* strain GV3101 pMP90 and transformed into *Arabidopsis* using the floral dip method. Oligonucleotide sequences for amplification of the various DNA fragments are listed in Table EV1.

Genotyping

To genotype the W10* *makr5* mutation, 215-bp genomic DNA fragments were amplified with primers 5′-GAA GCT CTT ACC TTT ATG AAA TAC TA-3′ and 5′-GTT GTT GTT TCG AGT CTC TG-3′ and then cut using SpeI restriction enzyme. When the $makr5^{W10*}$ mutation is absent, amplicons are cut into 25- and 190-bp fragments. To genotype *skm1* (SALK_087435) alleles, DNA fragments were amplified with primers 5′-ATG CAA ATG AAC TCG AGC TTC-3′ and 5′-TTC CGG TGA GAT TGT TGG TAG-3′ to detect wild type (1.05 kb), and 5′-ATT TTG CCG ATT TCG GAA C-3′ and 5′-TTC CGG TGA GAT TGT TGG TAG-3′ to detect the T-DNA insertion (600 bp). To genotype *skm2* (SALK_052069) alleles, DNA fragments were amplified with primers 5′-GTC AAG AGC TTC AAG CGA TTG-3′ and 5′-TTC CAG TTC CGA TCA CGT TAG-3′ to detect wild type (1.1 kb), and 5′-GTC AAG AGC TTC AAG CGA TTG-3′ and 5′-ATT TTG CCG ATT TCG GAA C-3′ to detect the T-DNA insertion (600 bp).

Fusion protein quantification

For quantification of *MAKR5::MAKR5-GFP*, *MAKR5::*$MAKR5^{1–206}$*-*$BKI1^{253–337}$*-CITRINE*, and *MAKR5::*$BKI1^{1–252}$*-*$MAKR5^{207–326}$*-CITRINE* fusion proteins, transgenic lines were grown in parallel until 5 dag and then transferred onto 20 nM CLE45 or mock for 3 h. Confocal microscopy images of corresponding protophloem cell files were taken and analyzed in ImageJ software (version 2.0.0.-rc-43/1.50e). Fluorescence intensity was measured as the mean gray value of a box-shaped region of interest, located either in the cytoplasm or centered on the rootward plasma membrane region of developing protophloem cells.

Quantitative real-time PCR (qPCR)

Total RNA was extracted from roots of 5-day-old seedlings using the RNeasy Plant Mini kit (Qiagen). One microgram of total RNA was used for reverse transcription (Invitrogen), and 1 μl of first-strand cDNA was used as a PCR template. qPCR analysis was performed using MESA BLUE qPCR MasterMix for SYBR (Eurogentec) with an Mx3000P qPCR machine (Agilent).

Expanded View for this article is available online.

Acknowledgements
We would like to thank Prof. H. Fukuda for the *skm1* and *skm2* mutants. This work was funded by Swiss National Science Foundation grant 310030B_147088 awarded to CSH.

Author contributions
YHK and CSH designed the study and wrote the paper together. YHK performed all experiments.

Conflict of interest
The authors declare that they have no conflict of interest.

References

1. Li J, Tax FE (2013) Receptor-like kinases: key regulators of plant development and defense. *J Integr Plant Biol* 55: 1184 – 1187
2. Zhu JY, Sae-Seaw J, Wang ZY (2013) Brassinosteroid signalling. *Development* 140: 1615 – 1620
3. Kinoshita T, Cano-Delgado A, Seto H, Hiranuma S, Fujioka S, Yoshida S, Chory J (2005) Binding of brassinosteroids to the extracellular domain of plant receptor kinase BRI1. *Nature* 433: 167 – 171
4. Li J, Chory J (1997) A putative leucine-rich repeat receptor kinase involved in brassinosteroid signal transduction. *Cell* 90: 929 – 938
5. Li J, Nam KH (2002) Regulation of brassinosteroid signaling by a GSK3/SHAGGY-like kinase. *Science* 295: 1299 – 1301
6. Yin Y, Wang ZY, Mora-Garcia S, Li J, Yoshida S, Asami T, Chory J (2002) BES1 accumulates in the nucleus in response to brassinosteroids to regulate gene expression and promote stem elongation. *Cell* 109: 181 – 191
7. Kim TW, Wang ZY (2010) Brassinosteroid signal transduction from receptor kinases to transcription factors. *Annu Rev Plant Biol* 61: 681 – 704
8. Wang X, Chory J (2006) Brassinosteroids regulate dissociation of BKI1, a negative regulator of BRI1 signaling, from the plasma membrane. *Science* 313: 1118 – 1122
9. Jaillais Y, Hothorn M, Belkhadir Y, Dabi T, Nimchuk ZL, Meyerowitz EM, Chory J (2011) Tyrosine phosphorylation controls brassinosteroid receptor activation by triggering membrane release of its kinase inhibitor. *Genes Dev* 25: 232 – 237
10. Wang H, Yang C, Zhang C, Wang N, Lu D, Wang J, Zhang S, Wang ZX, Ma H, Wang X (2011) Dual role of BKI1 and 14-3-3 s in brassinosteroid signaling to link receptor with transcription factors. *Dev Cell* 21: 825 – 834
11. Jiang J, Wang T, Wu Z, Wang J, Zhang C, Wang H, Wang ZX, Wang X (2015) The Intrinsically Disordered Protein BKI1 Is Essential for Inhibiting BRI1 Signaling in Plants. *Mol Plant* 8: 1675 – 1678
12. Xuan W, Audenaert D, Parizot B, Moller BK, Njo MF, De Rybel B, De Rop G, Van Isterdael G, Mahonen AP, Vanneste S *et al* (2015) Root Cap-Derived Auxin Pre-patterns the Longitudinal Axis of the Arabidopsis Root. *Curr Biol* 25: 1381 – 1388
13. Butenko MA, Simon R (2015) Beyond the meristems: similarities in the CLAVATA3 and INFLORESCENCE DEFICIENT IN ABSCISSION peptide mediated signalling pathways. *J Exp Bot* 66: 5195 – 5203

14. Rodriguez-Villalon A, Gujas B, Kang YH, Breda AS, Cattaneo P, Depuydt S, Hardtke CS (2014) Molecular genetic framework for protophloem formation. *Proc Natl Acad Sci USA* 111: 11551 – 11556
15. Depuydt S, Rodriguez-Villalon A, Santuari L, Wyser-Rmili C, Ragni L, Hardtke CS (2013) Suppression of Arabidopsis protophloem differentiation and root meristem growth by CLE45 requires the receptor-like kinase BAM3. *Proc Natl Acad Sci USA* 110: 7074 – 7079
16. Rodriguez-Villalon A, Gujas B, van Wijk R, Munnik T, Hardtke CS (2015) Primary root protophloem differentiation requires balanced phosphatidylinositol-4,5-biphosphate levels and systemically affects root branching. *Development* 142: 1437 – 1446
17. Endo S, Shinohara H, Matsubayashi Y, Fukuda H (2013) A novel pollen-pistil interaction conferring high-temperature tolerance during reproduction via CLE45 signaling. *Curr Biol* 23: 1670 – 1676
18. Scacchi E, Salinas P, Gujas B, Santuari L, Krogan N, Ragni L, Berleth T, Hardtke CS (2010) Spatio-temporal sequence of cross-regulatory events in root meristem growth. *Proc Natl Acad Sci USA* 107: 22734 – 22739
19. Beuchat J, Li S, Ragni L, Shindo C, Kohn MH, Hardtke CS (2010) A hyperactive quantitative trait locus allele of Arabidopsis BRX contributes to natural variation in root growth vigor. *Proc Natl Acad Sci USA* 107: 8475 – 8480
20. Briggs GC, Mouchel CF, Hardtke CS (2006) Characterization of the plant-specific BREVIS RADIX gene family reveals limited genetic redundancy despite high sequence conservation. *Plant Physiol* 140: 1306 – 1316
21. Deyoung BJ, Clark SE (2008) BAM receptors regulate stem cell specification and organ development through complex interactions with CLAVATA signaling. *Genetics* 180: 895 – 904
22. Santuari L, Scacchi E, Rodriguez-Villalon A, Salinas P, Dohmann EM, Brunoud G, Vernoux T, Smith RS, Hardtke CS (2011) Positional information by differential endocytosis splits auxin response to drive Arabidopsis root meristem growth. *Curr Biol* 21: 1918 – 1923
23. Gujas B, Alonso-Blanco C, Hardtke CS (2012) Natural Arabidopsis brx loss-of-function alleles confer root adaptation to acidic soil. *Curr Biol* 22: 1962 – 1968
24. Truernit E, Bauby H, Belcram K, Barthelemy J, Palauqui JC (2012) OCTOPUS, a polarly localized membrane-associated protein, regulates phloem differentiation entry in *Arabidopsis thaliana*. *Development* 139: 1306 – 1315

